

Development of an epitaxial growth process on European SiC substrates for a low leakage GaN

HEMT technology with power added efficiencies around 65%

P. Waltereit¹, S. Müller¹, L. Kirste¹, S. Storm², A. Weber², J. Splettstößer³, B. Schauwecker³

¹ Fraunhofer Institute for Applied Solid State Physics, Tullastrasse 72, 79108 Freiburg, Germany

² SiCrystal AG, Thurn-und-Taxis-Strasse 20, 90411 Nürnberg, Germany

³ United Monolithic Semiconductors GmbH, Wilhelm-Runge-Strasse 11, 89081 Ulm, Germany
phone: ++49 761 5159620, fax: +49 761 515971620, e-mail: patrick.waltereit@iaf.fraunhofer.de

Due to their wide band gap, high breakdown field, current density and saturation velocity, group III nitrides are well suited for high temperature and high power applications from RF to millimeter wave frequencies. SiC is the preferred substrate due to its high thermal conductivity, high resistivity as well as good lattice and thermal match to GaN.

Here we present an epitaxial growth process on semi-insulating 6H-SiC(0001) substrates from SiCrystal which is evaluated both on epiwafer level as well as on transistor level after subsequent device processing. For benchmarking at substrate, epitaxy and device level a comparison is carried out with epitaxial growth and processing performed in parallel on commercially available 4H-SiC(0001) substrates from Cree.

The bulk crystals from SiCrystal were grown by physical vapour transport. Substrates with around 360 μm thickness were cut from the boule and polished on both sides. The SiC substrates are structurally, electrically and thermally characterized by cross-polarizer imaging, x-ray diffraction and contactless resistivity measurements. The cross-polarizer images (Figure 1) reveal a higher degree of strain inhomogeneity for the SiCrystal substrates compared to Cree material. This result is confirmed by x-ray rocking curves of symmetric 4H-SiC 00.8 and 6H-SiC 00.12 substrate reflections. The substrates resistivities are around $10^{10} \Omega \times \text{cm}$ for both types of SiC substrates. However, we detect different activation energies around 0.8 and 1 eV for SiCrystal and Cree substrates. Additionally, we measure slightly different thermal conductivities of 420 and 400 $\text{W m}^{-1} \text{K}^{-1}$ for Cree and SiCrystal substrates.

The growth of the AlGaIn/GaN HEMT structure is performed in a 12×3-inch multiwafer reactor at Fraunhofer IAF. Growth on the SiC substrates is initiated by a thin AlN nucleation layer followed by a 1.8 μm thick GaN buffer that consists of a bottom Fe-doped and a top undoped part in order to achieve both high buffer resistivity as well as a low trap concentration near the 2DEG region. The barrier and the cap layer of the HEMT structure consist of a 22 nm $\text{Al}_{0.18}\text{Ga}_{0.82}\text{N}$ barrier and a 3 nm GaN cap. Figure 2 shows a sheet resistance mapping, evidencing a homogenous two-dimensional electron gas. The barrier thickness and composition was determined by high-resolution x-ray diffraction in conjunction with dynamical simulations, see Figure 3 left. For similar nominal structures it was necessary to perform individual growth runs for both substrate types. For instance, special attention was paid to substrate differences such as the different thermal conductivities of SiCrystal and Cree substrates leading to different surface temperatures (10 K lower for SiCrystal substrates in our machine) during growth. This effect results in lower Al-contents (about 2.5% absolute) and thicker AlGaIn layers (about 3 nm) on SiCrystal substrates w.r.t. Cree substrates when growing on both substrate types simultaneously. The growth conditions of the AlN nucleation layer and of the GaN buffer were optimized for a low dislocation density (low 10^8 cm^{-2} range as determined by plan-view transmission electron microscopy), smooth surfaces (root mean square roughness well below 0.2 nm over an $2 \times 2 \mu\text{m}^2$ area, see Figure 3 center), and low carrier concentration in the buffer (Figure 3 right) and high buffer isolation (above $10^{12} \Omega/\text{sq}$). We do observe differences in the high-resolution x-ray diffraction ω -scan 00.2 and 10.2 GaN linewidths, namely around 0.04° and 0.03° in the (002) reflection and 0.05° and 0.07° in the (102) reflection for Cree and SiCrystal substrates, respectively. We assume this difference is due to the different nucleation on 4H and 6H substrates.

Device processing of several iterations of epitaxial material is carried out using the qualified GH50 technology (for applications up to 7 GHz) from United Monolithic Semiconductors. We do observe an improvement in sheet resistance, drain saturation current and threshold voltage (see Figure 4) towards achieving homogeneous distributions within the target range which we attribute to optimizations of the epitaxial growth process. The level of leakage at 50 V drain bias is around $10 \mu\text{A}/\text{mm}$ (see Figure 5) and remains below $100 \mu\text{A}/\text{mm}$ up to the highest voltage of 150 V tested. Loadpull measurements at 50 V drain bias and 2 GHz operating frequency yield a power density of 5 W/mm and a power added efficiency around 65% when tuned for optimum power and efficiency, respectively, see Figure 6. These values are achieved on both substrate types (although a slight trend to lower PAE is visible for SiCrystal substrates), indicating that we have indeed realized epitaxial material of very similar high quality on both SiCrystal and Cree substrates.

Keywords: GaN, SiC, HEMT

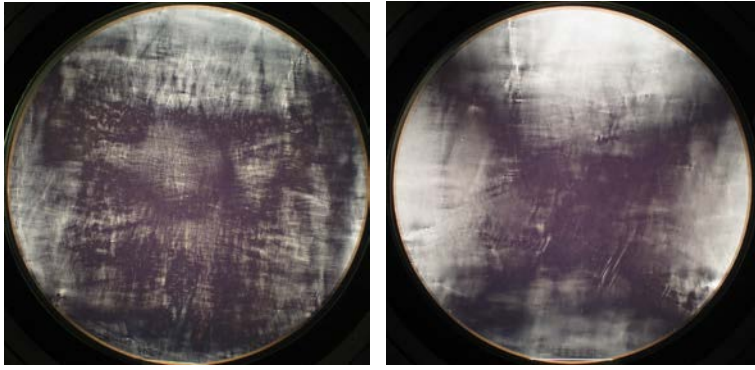


Figure 1: Cross-polarizer images of a SiCrystal (left) and a Cree (right) substrate indicating a higher degree of strain inhomogeneity on SiCrystal substrates.

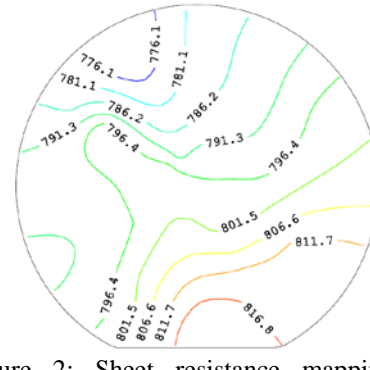


Figure 2: Sheet resistance mapping of an $\text{Al}_{0.18}\text{Ga}_{0.82}\text{N}/\text{GaN}$ epitaxial structure grown on SiCrystal substrate: $797 \Omega/\text{sq} \pm 1.4\%$

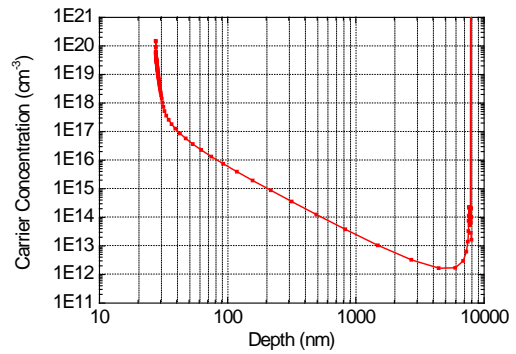
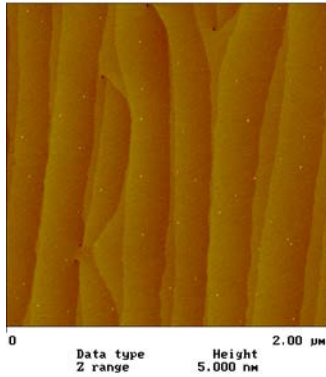
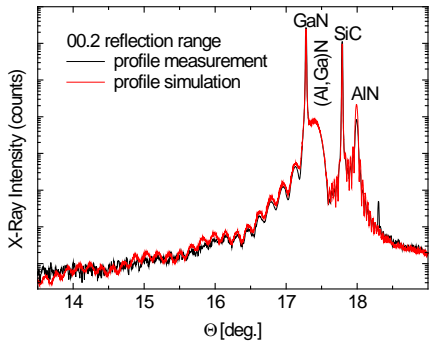


Figure 3: X-ray diffraction profile (left), atomic force micrograph (center) and depth-profile of carrier concentration from capacitance-voltage profiling (right). The depth information near the substrate is limited by the measurement accuracy.

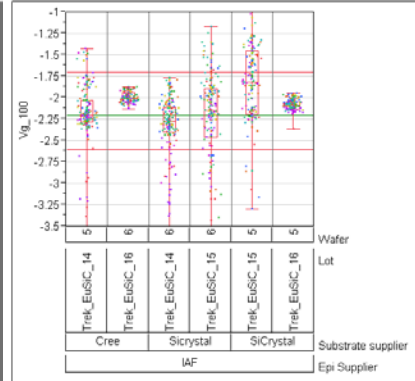
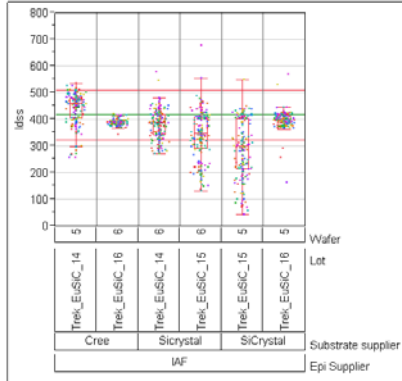
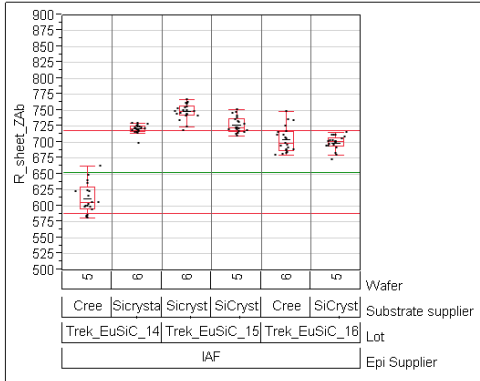


Figure 4: Sheet resistance (Ω/sq), drain saturation current (mA/mm , $U_{\text{GS}}=0 \text{ V}$) and threshold voltage (V , defined by 1% of I_{dss}) of transistors processed on AlGaIn/GaN epitaxial layers fabricated on SiCrystal and Cree substrates. The variations from wafer to wafer originate from varying Al-contents during optimization of the growth process.

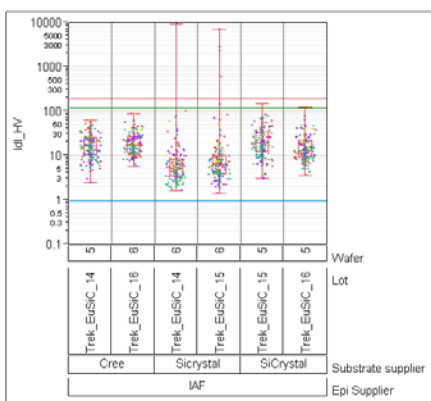


Figure 5: Drain leakage current ($\mu\text{A}/\text{mm}$) at 50 V drain bias.

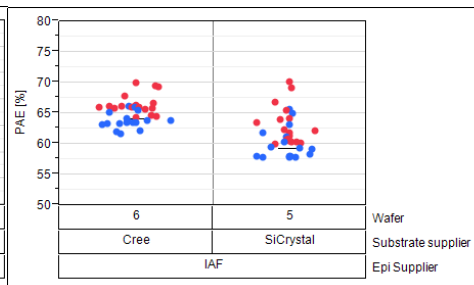
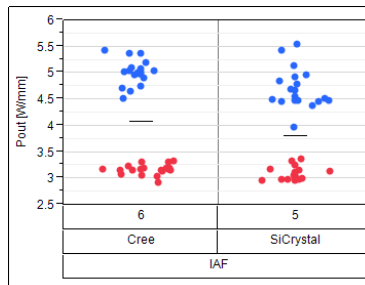


Figure 6: Output power density (W/mm , left) and power added efficiency ($\%$, right) from loadpull measurements at 50 V drain bias and 2 GHz operating frequency. The blue and red data points correspond to optimum tuning for power and efficiency, respectively.